Levelized Cost of Storage for Li-Ion Batteries Used in PV Power Plants for Ramp-Rate Control

Hector Beltran, Iván Tomás García, José Carlos Alfonso-Gil, and Emilio Pérez

***Abstract*—Photovoltaic (PV) power production ramp-rate control is getting more and more important in weak electric power systems, in which quick and significant power fluctuations can affect the stability of the system. This can be achieved by means of the integration of batteries into large PV plants but such an operation involves an aggressive environment for the ageing of the batteries. This paper presents an evaluation of this ageing by means of the annual simulations of a large PV power plant using actual irradiance data. This is done for different battery sizes used under various degrees of limitation in the power ramp-rate variation. The levelized cost of storage is calculated for each of the cases considered.**

***Index Terms*—Photovoltaic power plants with energy storage, ramp-rate control, batteries, ageing analysis.**

I. Introduction

The power fluctuations experienced by Photovoltaic (PV) power plants as a consequence of the low, fast-moving clouds over them is one of the most important challenges for the massive integration of this technology in the electric power system. Since clouds' impacts are highly localized effects, this handicap has been typically minimized thanks to the general dispersion of PV generators in a wide area region [1]. However, the growing development and penetration of large scale PV installations in weak or isolated power grids is posing new challenges for the corresponding electric power system operators. The challenges are mainly associated to the grid stability because these systems are usually not very vast. Then, when a significant part of the energy production is highly variable, the system operators have to define or impose certain restrictions to the stochasticity of the PV production. This is being faced by certain operators such as the Puerto Rico Electric Power Authority (PREPA, [2]), the Hawaiian Electric Company (HECO, [3]), or the Faroe Islands utility (SEV, [4]) all of them good examples of weak grids. The solution being defined is based in the introduction of certain ramp-rate power limitations that restrict the variation of the PV production over short-periods of time. This can be achieved with the integration in the PV power plants of some type of energy storage system, mainly batteries, Fig. 1. Various proposals are available in the literature that analyze their use under this ramp-rate power control strategy [5]–[10], and even the use of ultracapacitors for it [11]. Similar proposals are done by other authors for wind power plants with storage [12]–[15].

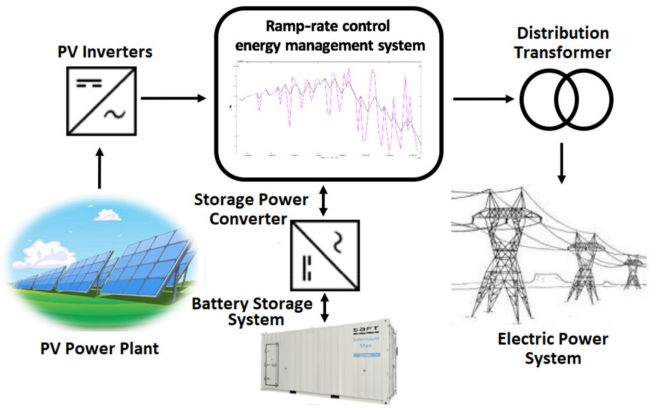

Fig. 1. Scheme of the PV plant with batteries for power ramp-rate control.

Therefore, it is the role of the energy storage system (batteries) operating within the renewable energy source power plant to cope with the power difference during the periods in which the PV panels have stochastically and rapidly varied their production and must inject into the grid a given limited production while the PV panels produce differently. In this way, the ramp-rate control achieved thanks to the introduction of batteries in a renewable energy power plant implies a more or less continuous mode of operation in which the batteries are being charged and discharged over and over. This involves ageing the batteries accordingly. Multiple authors have analyzed the ageing mechanisms associated to the batteries under different stress factors [16]–[21], and propose different types of models to evaluate it and perform some type of prognosis [22]–[27].

Although different authors have faced the PV power ramp-rate control strategy using batteries, it is important to highlight that these mainly focus on the definition of new control algorithms that usually pursue either the minimization of the size of the batteries (energy capacity requirements) or the optimized operation of the PV plant with storage. Moreover, the references cited for battery ageing are mainly associated to the electric vehicle industry. Therefore, none of the previous works has investigated the impact on the ageing of the batteries produced by the power ramp-rate limitation strategy when implemented in a PV power plant. This work presents such an evaluation by

Manuscript received March 29, 2018; revised October 23, 2018; accepted December 20, 2018. This work was supported by Universitat Jaume I through its special program to foster the scientific research and the technological development under Grant UJI-B2017-26. Paper no. TEC-00322-2018. *(Corresponding author: Hector Beltran.)*

The authors are with the Department of Industrial Systems Engineering and Design, Universitat Jaume I, Castelló de la Plana 12071, Spain (e-mail: hbeltran@uji.es; al190105@uji.es; jalfonso@uji.es; pereze@uji.es).

Color versions of one or more of the figures in this paper are available online at http://ieeexplore.ieee.org.

Digital Object Identifier 10.1109/TEC.2019.2891851

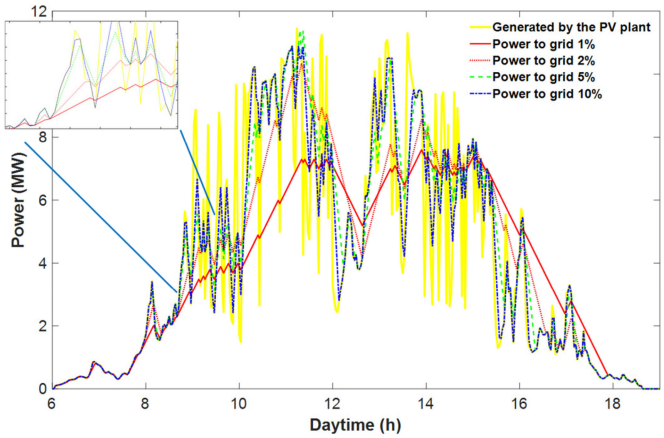

Fig. 2. Power production of the 10 MW PV plant with batteries under different degrees of ramp-rate limitation (defined in % in the legend).

means of annual simulations of a large PV power plant (10 MW) using actual irradiance data. This is done for different sizes of batteries used under various degrees of limitation in the power ramp-rate variation. The Levelized Cost of Storage (LCOS) is calculated for each of the combinations.

Then, after discussing about the potential type of Li-ion battery to be used in such an application in Section II, and the stress factors that can affect their lifetime in Section III, the current work analyzes in Sections IV and V the ageing experienced by the batteries taking into account both calendar and cycle ageing models. The paper concludes with the estimation of the LCOS and some final remarks.

II. PV Power Ramp-Rate Control With Batteries

Due to the inherent fluctuation of the PV power production associated to the transient clouds, which can achieve values beyond 90% and 70% for 1 MW and 10 MW PV plants in one single minute, respectively [28], some electric system operators controlling weak power grids are starting to impose some limitations to the production variability of this renewable technology. As already introduced in the previous section, this is a well stablished and known control proposal defined in various electric codes and implemented in actual systems to avoid stability problems. Also in the literature, different authors have analyzed this solution for PV plants and defined some variations intended to: minimize the size of the batteries involved [6], [7], [10], [28], to perform some supervisory control over the operation of the combined "PV + storage" plants [8], or to optimize the size of the potential second-life batteries to be used with this goal [9].

We analyze in our work four different degrees of power ramp-rate variation, the cases in which the PV power plant production with batteries is allowed to modify its production every minute no more than 1%, 2%, 5%, and 10%, with regard to its PV rated power, Fig. 2. These limitation levels correspond to the usual control levels defined in the grid codes that already demand it (mostly 10%) and to potential more restrictive levels (<10%) to be fixed in the coming future. In this sense, the lower the power variation allowed (in %), the higher the degree of filtering introduced by the batteries and, accordingly, the deeper the charge-and-discharge cycling pattern experienced with the consequent ageing. The depth-of-discharge of the cycles will be also function of the battery energy capacity, which will be analyzed in between 1 and 10 MWh for the 10 MW rated power PV plant under consideration. These energy capacity values are based on the characteristics of the existing installations.

Regarding the type of batteries, up to six different families are commercialized nowadays: Lithium Cobalt Oxide (LCO or LiCoO2), Lithium Iron Phosphate (LFP or LiFePO4), Lithium Nickel Cobalt Aluminium Oxide (NCA or LiNiCoAlO2), Lithium Manganese Oxide (LMO or LiMn2O4), Lithium Nickel Manganese Cobalt Oxide (NMC or LiNiMnCoO2), and Lithium Titanate (LTO or Li4Ti5O12). These mainly differ in the material constituting the cathode. Only the LTO family associates its name to the anode's material, being in all the cases the second electrode made of graphite. The operational characteristics also differ being NCA the one with highest specific energy; however, LFP and LTO are superior in terms of specific power, cyclability, and thermal stability, what makes them appropriate for intensive power demanding applications such as ramp-rate control. LTO also presents the best life span although it is the most expensive technology. In all, since space is not a limiting parameter for this type of installation and price is lower than for other lithium types, LFP is the selected chemistry for our analysis. Note in this regard that it is being developed and installed by companies such as SAFT Batteries for ramp-rate control applications in wind farms [29].

III. Battery Ageing Stress Factors and Model

The ageing phenomenon of Li-ion based batteries has been extensively analyzed in the literature in the last years due to its importance not only for the renewables' integration expansion but mainly for the electric vehicle continuously increasing industry. In this sense, the multiple ageing models and analyses performed have been classified by different authors [30]–[33] into 2 main groups: performance-based lifetime models, and post-processing models. The way to analyse the ageing differs in the different works, however, the resulting stress factors are quite coherent among publications for the various battery chemistries analysed.

A. Battery Ageing Stress Factors

The identified stress factors that influence the ageing of Li-ion batteries can be mainly listed as: time, temperature, state-of-charge (SOC) during rest, number of cycles experienced, depth-of-discharge (DoD) of the cycles, average voltage of the cycles, and charge/discharge current rate.

Their corresponding influence depends on the type of battery and on the design under consideration and is usually studied according to two types of mechanism: calendar and cycle ageing. Then, while the calendar ageing is usually associated to the capacity reduction of the batteries as a function of time without being cycled (only by being connected in hot stand-by), the cycle ageing is associated to their continuous use (by being charged and discharged). In this sense and for the case of Li-ion

batteries, the calendar ageing gets generally more significant with time as temperature and SOC are higher [16]–[20]. The relation with temperature is normally modelled by means of the Arrhenius equation (1) while the dependence over the voltage (or SOC) is generally less important and follows a polynomial or even linear relation, depending on the lithium battery type.

$$k\left(t\right) = A \times e^{-\frac{Ea}{RT}} \tag{1}$$

With regard to the cycle ageing, this is highly influenced by the number of cycles experienced [22]. The DoD of the cycles is also important, having a lower ageing effect with shallower depth cycles [17], [22], as it is important to perform the cycles as close as possible to the 50% of SOC to minimize the ageing impact due to the average voltage during the cycling [18], [23]–[26]. Finally, also the temperature significantly affects the cycle ageing [21], [25]–[27] what forces most battery manufacturers to advice their use under refrigerated conditions not much above 25 °C. After all, it can be concluded that both effects (calendar and cycle) are important and dependent on the combination and degree of the stress factors [16]. Therefore, none of them can be disregarded in a thorough full research.

B. Ageing Model Used for Analysis

As discussed previously, due to the application under study (power rate-ramp control for a large PV plant), the use of LFP batteries is analysed. Therefore, among the multiple Li-ion equivalent model proposals, only some of those focused on this chemistry have been considered in depth [18], [19], [23], [25], [34]–[38]. And among them, since some have been developed based on electric vehicle (EV) standard drive cycle profiles, only those from Stroe [18], Swierczynski [23], and Weißhar [38] are considered appropriate for our analysis. These authors propose different ageing models for LFP batteries combined with renewable energy plants. However, the latter applies them for small domestic installations. Therefore, due to the similarity with the type of application analysed in Stroe [18] for wind power plants, the present work uses the model proposed by this author to analyse how LFP batteries are going to lose capacity over time when used for power rate-ramp control in a large PV plant. This model is based on the following semi-empirical equations defined for both capacity fades (in %) associated respectively to the calendar and the cycle ageing:

$$C_{fade,cal}\left(t,T\right) = \alpha_t \times e^{\beta_t \cdot T} \times t^n \tag{2}$$

$$C_{fade,cyc}\left(NC,T\right) = \alpha_{NC} \times e^{\beta_{NC} \cdot T} \times NC^n \tag{3}$$

Where t is the time in months, T is the temperature in Kelvin, and NC represents the number of equivalent reference cycles. The coefficients in these equations are $\alpha_t = 3.087 \cdot 10^{-7}$, $\alpha_{NC} = 6.87 \cdot 10^{-5}$, $\beta_t = 0.05146$, $\beta_{NC} = 0.027$, and n = 0.5, for both equations. Note that the C-rate stress factor influence is not included in the model because C-rates below 4C are considered in the application analysed in our work. Under these operating conditions, the C-rate influence can be neglected [39].

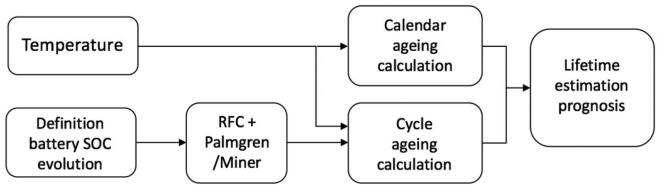

Fig. 3. Structure of the methodology implemented to analyze the LFP battery capacity fade along the ramp-rate control operation.

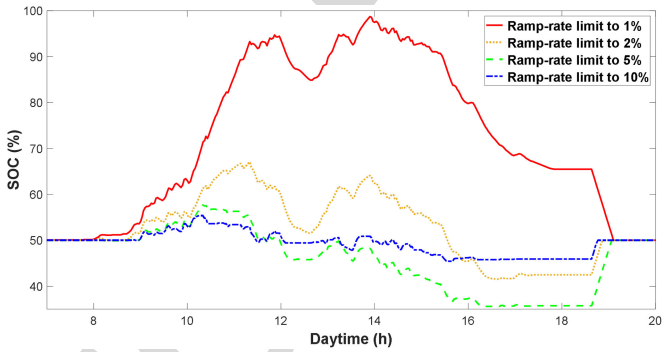

Fig. 4. State-of-charge evolution of the 5 MW battery under different degrees of ramp-rate limitation for the day represented in Fig. 2.

IV. Analysis of the Ageing Under Ramp-Rate Control

This analysis is based on the ageing model introduced in the previous section which is combined in this work with the rainflow-counting (RFC) algorithm [40]–[42] and the Palmgren-Miner rule [22], [43]–[45]. In this way, the proposed hybrid methodology provides an estimation of the lifetime expectancy of the batteries under the power ramp-rate control regime of operation.

A. Methodology Implemented for the Ageing Prognosis

The methodology developed to analyze the ageing is summarized in Fig. 3, where the scheme interrelating the inputs, the calculation/simulation steps, and the final output is shown.

Then, the proposed analysis model presents various stages that can be clearly observed. First, the evolution of the SOC of the battery experienced along one whole year operating under the ramp-rate control regime is generated. As can be observed in Fig. 4 for the day whose power exchanges are represented in Fig. 2, this is done for four different degrees of ramp rate control limitation (1%/min, 2%/min, 5%/min, and 10%/min), introducing in all the cases a programmed SOC recovery of its initial value (50%) after the battery daily operation.

The analysis in this work is also performed for various battery sizes (from 1 MWh up to 10 MWh), for two extreme potential roundtrip efficiencies of the batteries (85%, and 92%), and for two different operating temperatures (25 °C and 35 °C), at which the batteries are considered to be refrigerated on-site. The battery exchange power capacity is always considered the same and defined as 5 MW, according to recommendations from SAFT for this specific application.

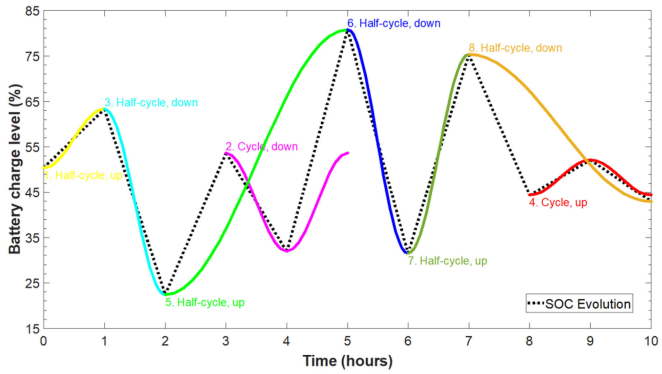

Fig. 5. Adaptation performed by the RFC MATLAB function to the SOC evolution to account the number of half cycles and their DoD.

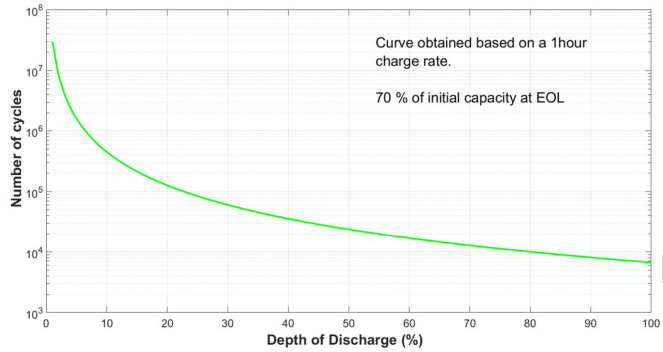

Fig. 6. Cycles to failure vs. DoD curve for LFP batteries from SAFT.

Then, following the scheme, the SOC evolution curve is introduced into the RFC algorithm which processes the SOC curve as represented in Fig. 5. This returns the number of cycles experienced by the battery at varying DoDs, as well as the medium voltage for each partial charge/discharge cycle.

This information is then handled by the Palmgren-Miner rule (4) which compares the partial cycling histogram provided by the RFC with the maximum number of cycles that the battery could perform at each single DoD. This equation dispenses the degradation (D) experienced over the simulated time period:

$$D(\%) = \sum_{DoD=1}^{DoD=100} \frac{N_{cyc}\,(DoD)}{N_{\max}\,(DoD)} \tag{4}$$

Where N_{cyc} is the number of cycles returned by the RFC algorithm and experienced for each amplitude (defined by the *DoD* variable), and $N_{\max}$ is the number of cycles the battery can withstand for each specific DoD, according to the capacity evolution curves of the batteries provided by the manufacturer. Fig. 6 plots this curve for the case of the Intensium Max High Power VL30P cells type from SAFT batteries, which can be approximated by the following equation (5):

$$N_{\max}\,(\mathrm{DoD}) = 3 \cdot 10^7 \times DoD(\%)^{-1.825} \tag{5}$$

The degradation parameter D calculated in (4) is useful to estimate the number of equivalent reference cycles (*NC*) that the battery has experienced over the year. As deduced from

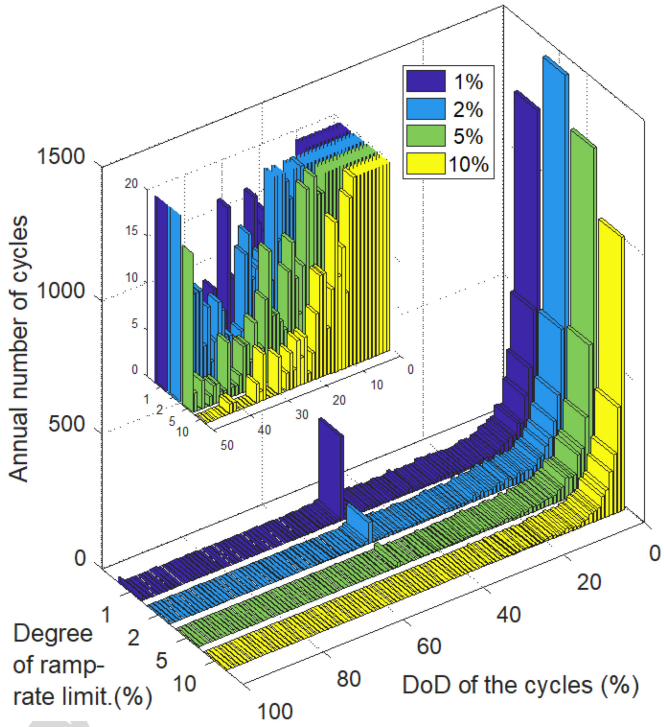

Fig. 7. Histograms representing the annual cycling pattern of a 5 MW / 5 MWh battery under the four different degrees of ramp-rate limitation, with a zoom over the range 0–50% in DoD of the cycles and up to 20 accumulated cycles.

Fig. 6, these LFP batteries can withstand around 10000 cycles at 80% DoD, what means that the *NC* can be calculated as (6).

$$NC\,(@80\%) = \frac{D\,(\%) \times 10000}{100\%} \tag{6}$$

Thereafter, once accounted the *NC*, this information is introduced into equations (2) and (3) together with the temperature. The resulting capacity fade values are combined to finally provide the lifetime estimation prognosis, in years, by means of equation (7) which takes into account that the battery manufacturer defines the end-of-life (EOL) of the batteries when the retained capacity (*RC*) is the 70% of its initial value.

$$RC = \{1 - [C_{fade,cal}\,(y_{EOL}, T) + C_{fade,cyc}\,(NC, T) \times y_{EOL}]\} \tag{7}$$

The solution in years (y_{EOL}) at this equation is the estimated lifetime of the battery (EOL time). All the procedure has been implemented and automated in Matlab/Simulink which presents a RFC library that simplifies part of the programming.

B. Results of the Ageing Analysis

Annual simulations of a 10 MW PV power plant using actual irradiance data have been performed to avoid seasonal effects for all the cases described in the previous sections (different filtering levels, various battery energy capacity sizes, and two operating temperatures). The simulations have been done with a one-minute time step, what provides a good track of the fast power fluctuations. Then, the obtained SOC evolution of the various batteries were treated with the RFC algorithm to derive the cycling histograms as the one represented in Fig. 7.

TABLE I
LIFETIME ESTIMATION (IN YEARS) FOR A ROUNDTRIP EFF. = 85%

Temp = 25ºC

Capacity \ Filt.	1%	2%	5%	10%
1 MWh	3.18	3.38	4.22	5.42
2 MWh	3.98	4.26	5.62	7.69
3 MWh	4.22	5.01	6.89	9.42
4 MWh	4.59	5.48	8.00	11.2
5 MWh	4.98	6.08	8.98	12.6
6 MWh	5.08	6.65	9.75	14.0
7 MWh	5.32	7.12	10.6	15.1
8 MWh	5.72	7.70	11.4	16.1
9 MWh	6.02	8.20	12.2	17.0
10 MWh	6.23	8.70	13.0	17.7

Temp = 35ºC

Capacity \ Filt.	1%	2%	5%	10%
1 MWh	2.06	2.15	2.65	3.30
2 MWh	2.35	2.70	3.34	4.36
3 MWh	2.69	3.05	4.04	5.28
4 MWh	2.92	3.30	4.48	6.07
5 MWh	3.02	3.66	5.05	6.65
6 MWh	3.09	4.00	5.35	7.17
7 MWh	3.24	4.18	5.85	7.57
8 MWh	3.38	4.38	6.18	8.01
9 MWh	3.59	4.71	6.42	8.26
10 MWh	3.79	5.01	6.82	8.50

TABLE II
LIFETIME ESTIMATION (IN YEARS) FOR A ROUNDTRIP EFF. = 92%

Temp = 25ºC

Capacity \ Filt.	1%	2%	5%	10%
1 MWh	3.15	3.35	4.12	5.35
2 MWh	3.92	4.20	5.44	7.42
3 MWh	4.16	5.00	6.68	9.28
4 MWh	4.50	5.38	7.76	11.0
5 MWh	4.89	6.01	8.67	12.3
6 MWh	5.05	6.42	9.42	13.6
7 MWh	5.26	7.05	10.3	14.8
8 MWh	5.59	7.44	11.2	15.7
9 MWh	6.00	8.05	12.0	16.6
10 MWh	6.11	8.41	12.7	17.4

Temp = 35ºC

Capacity \ Filt.	1%	2%	5%	10%
1 MWh	2.05	2.11	2.58	3.27
2 MWh	2.34	2.67	3.29	4.32
3 MWh	2.66	3.02	4.01	5.23
4 MWh	2.89	3.27	4.38	6.01
5 MWh	3.01	3.58	5.00	6.50
6 MWh	3.07	3.95	5.28	7.08
7 MWh	3.20	4.10	5.70	7.42
8 MWh	3.33	4.32	6.08	7.88
9 MWh	3.50	4.59	6.34	8.17
10 MWh	3.71	4.91	6.67	8.38

By applying the rest of the analysis methodology to these histograms, the ageing prognosis for the multiple case studies is obtained. The resulting lifetime estimation to achieve the 30% drop in energy capacity is summarized in Table I and Table II, for the roundtrip efficiencies of 85% and 92%, respectively, and for the two temperatures considered.

Results indicate that improving the roundtrip efficiency of the battery from 85% up to 92% on the AC side of the energy storage system has not significant effect to the battery ageing. On the contrary, operating the battery at 35 °C instead of 25 °C represents a potential life span reduction varying from 40% to 60%. Therefore, it is clear that the operation temperature of the battery cells should be kept under control and as close as possible to the 20–25 °C recommended by manufacturers. Although not summarized on these tables, further simulations performed for 20 °C confirm lifetime can be further extended by another 20–25% at this temperature. With regard to the degree of control of the ramp-rate variations, it stands out how the more restrictive the control is (lower percentage of variation allowed) the shorter the lifetime expectancy because the battery is more demanded. Finally, note how, similarly, the increasing energy capacity of the battery favors the extension of its lifetime due to the shallower cycles experienced throughout the annual operation for a given power exchange pattern with the grid.

Further conclusions can be obtained from the graphical representation in Fig. 8. This shows for different operation conditions the capacity fades associated to the calendar (red) and to the cycling (blue) ageing mechanisms, which add up the 30% fade of the initial battery capacity accepted by the manufacturer as EOL (70% of capacity retention). Although the cycle ageing is generally assumed to be more important than the calendar one, it is straightforward derived from Fig. 8 that both types of ageing mechanisms are significant and both have to be taken into consideration in this application for the design and sizing definition of the battery to guarantee a proper lifetime. Note how their corresponding weight on the overall ageing of the battery is clearly dependent on the battery size and on the filtering level, since these two design parameters condition the DoD of the cycles experienced during the annual operation. It is therefore important to highlight that histogram results in Fig. 7 together with the surfaces represented in Fig. 8 demonstrate that the ramp-rate control strategy analyzed in this work is not a very demanding energy management strategy for batteries used in a PV power plant from a cycle ageing mechanism point of view. Clearly, the calendar ageing is also significant in this application and cannot be despised. Finally, note that the progressive reduction of the battery capacity with time and use will imply a lower and lower capability to control the ramp-rate as the EOL of the battery approaches.

V. ESTIMATION OF THE LEVELIZED COST OF STORAGE

Once the ageing of the batteries has been quantified, it is necessary to identify a valid method to define or calculate the relative and comparable costs of the different battery solutions analyzed to provide the ramp-rate control service. Energy storage systems that are implemented as a way to improve the management capability and the quality of the energy discharged to the grid pose a complex problem to quantify its benefits and effectiveness with respect to their cost. This is due to the fact that they do not produce electricity from an energy source, but store it for a time, and to the interrelation that exists among all the aspects that take part in their operation. All of this makes the evaluation difficult with a simple analysis.

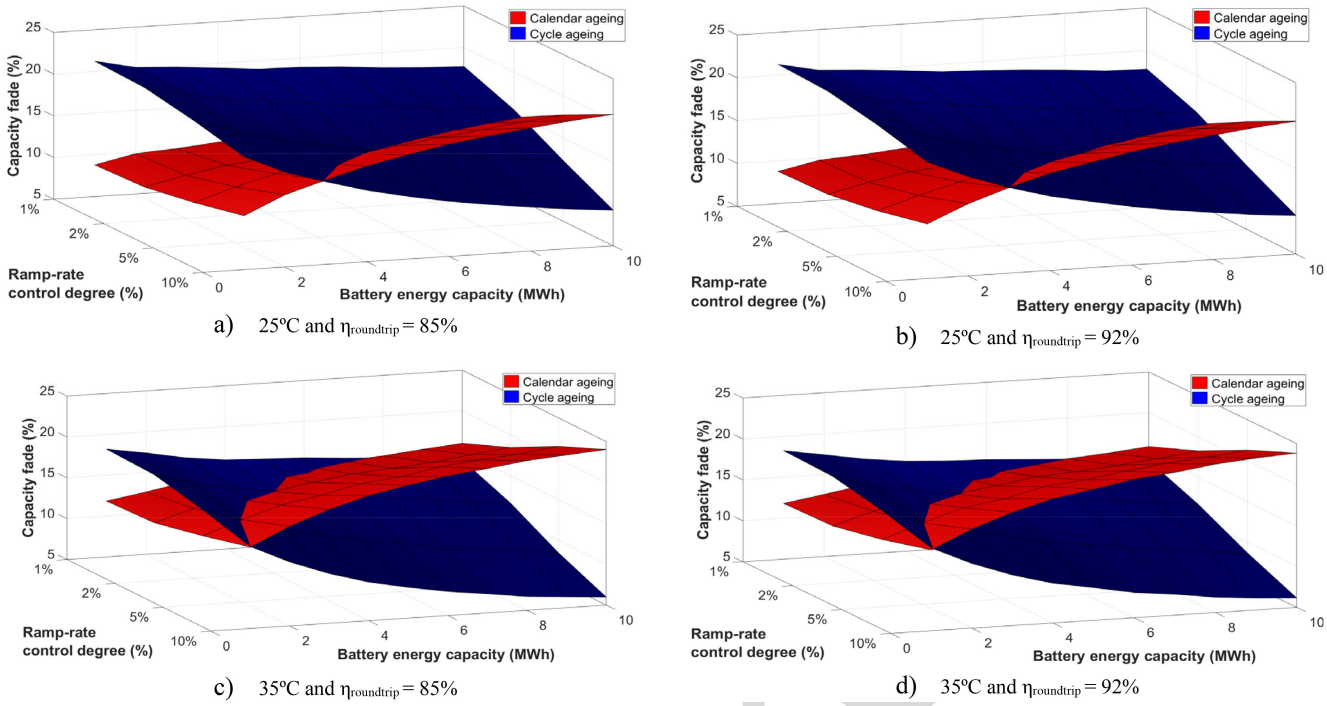

Fig. 8. Capacity loss (in %) experienced by a 5 MW battery at 25 °C [a) and b)] and 35 °C [c) and d)] for the two roundtrip efficiencies under consideration.

Levelized Cost of Storage (LCOS) is an innovative tool [46] derived from the traditional LCOE calculation [47], used to compare the lifetime cost of the energy producing technologies, but adapted to energy storage systems that do not produce energy by themselves but store it for a later use introducing some energy losses. Therefore, LCOS is being used to compare the cost of using different storage technologies along their lifespan for a given application in the electric power sector. In this sense, LCOS can be defined as the cost per usable energy storage capacity throughout the lifetime of the installation. This is calculated, according to [46], taking into account the initial investment of the system, plus all the operating and maintenance costs accumulated during its use, divided by the so-called lifetime utilization factor (LUF), as in (8):

$$LCOS_{EOL} = \frac{I_o + \sum_{y=0}^{EOL} Op_{cost}}{\sum_{y=0}^{EOL} C_y \times \sqrt{\eta_y} \cdot \Delta t} \ (€/\text{kWh per year}) \quad (8)$$

Where the different parameters involved are:

- *EOL*, lifetime expectancy in years, according to the analysis introduced in the previous section.
- I_o, initial investment cost of the whole energy storage system (batteries, converters, cooling unit, protections and control equipment . . .), in €/kWh.
- Op_{cost}, overall operating annual cost (maintenance, security, recharge costs, auxiliary power, control and management). This is usually accounted for as a percentage of the initial investment, also in €/kWh.
- C_y, energy capacity of the battery let at year "y" with regard to its initial value (100%-degradation), in %.
- η_y, battery roundtrip AC-to-AC efficiency, in %.
- Δt, the incremental time, in years.

TABLE III
INITIAL INVESTMENT COST OF THE 5 MW BATTERIES (IN M€) FOR THE DIFFERENT BATTERY CAPACITIES TAKEN INTO ACCOUNT

1 MWh	2 MWh	3 MWh	4 MWh	5 MWh
1.45	1.9	2.35	2.8	3.25
6 MWh	7 MWh	8 MWh	9 MWh	10 MWh
3.27	4.15	4.6	5.05	5.5

For this calculation, the initial investment cost has been introduced according to that in Table III for the different battery energy capacities. These costs are based on the average price per kW and kWh of installed LFP battery (including all the equipment) registered and estimated in various reports from different international technology centers and specialized consultancies [48]–[51]. The overall operating annual costs has been assumed to be the 3.5% of the initial investment, upon estimations from battery manufacturers. An annual monetary discount rate equal to 4% is also assumed. The annual capacity left in the battery is updated every year as a function of the calculated degradation parameter. As it is done with the one-way efficiency which is initially taken as 96% (corresponding to the roundtrip efficiency of 92% previously analyzed). The case of the 85% roundtrip efficiency has not been calculated due to the low impact reflected on the ageing that has been already discussed.

Therefore, according to (8) and taking into account the ageing results and estimated lifetimes presented before, Table IV summarizes the LCOS calculated values at the EOL of the batteries for the different combinations of parameters that have been considered at both 25 °C and 35 °C. It is notably remarkable

TABLE IV
LCOS OF THE 5 MW BATTERIES BASED ON THE ESTIMATED EOL (IN €/KWH)

Temp = 25ºC

Capacity \ Filt.	1%	2%	5%	10%
1 MWh	665	630	512	403
2 MWh	352	330	261	197
3 MWh	275	230	179	134
4 MWh	229	194	140	111
5 MWh	196	162	118	88
6 MWh	180	146	104	77
7 MWh	167	128	96	69
8 MWh	154	119	84	64
9 MWh	140	108	78	59
10 MWh	135	102	73	56

Temp = 35ºC

Capacity \ Filt.	1%	2%	5%	10%
1 MWh	1020	997	785	644
2 MWh	597	523	420	394
3 MWh	433	372	283	222
4 MWh	350	311	235	174
5 MWh	309	265	191	152
6 MWh	289	227	174	133
7 MWh	268	210	156	124
8 MWh	251	195	142	113
9 MWh	234	180	134	107
10 MWh	216	165	126	103

from the results that although the initial investment cost obviously influences the LCOS value of the system, the increase in the estimated service life of the batteries, due to a less stressing operation regime and the consequent reduced ageing, involves a decrease in the resulting LCOS of the larger energy capacity batteries. Therefore, the larger the capacity, the lower the LCOS in this application. Still, the operating temperature is also very important since the LCOS can vary for the same battery and ramp-rate limitation level between 40 and 50% for operating temperatures going from 25 °C up to 35 °C.

Finally, note that results presented in this work can be compared with those provided by the financial advisory and asset management firm Lazard in [52]. This consultancy offers LCOS values ranging from $272 up to $386 for "in-front-of-the-meter" applications. Therefore, some of the combinations analyzed here offer a LCOS quite lower than those estimated by Lazard. However, this is mainly obtained for large capacity batteries that, although taken into account here, would be difficult to justify for the ramp-rate control application from an economic and financial point of view.

VI. CONCLUSIONS

In conclusion, the ramp-rate PV power production control is a grid injection power limitation that is gaining importance in the electric systems, mainly in weak power systems to the moment, as the degree of penetration of PV power plants gets higher. The inherently intermittent and stochastic power production fluctuations of this technology could affect the stability of the system. This limitation can be managed by integrating batteries into large PV plants but such an operation involves an aggressive environment for the ageing of the batteries. This work has analyzed this ageing for a specific technology of lithium ion batteries, the LFP family. Results in this sense highlight the importance of the temperature of operation of the batteries as well as the influence of the battery size and degree of ramp-rate limitation on the cycle ageing. Lifetime estimations range from 3.6 years up to 12.2 years depending on the battery size and the ramp-rate control at 35 °C. This ageing prognosis opened the door to a careful analysis of the Levelized Cost of Storage for this application using batteries. In this sense, LCOS results are in accordance with previous reports and tend to offer optimistic low cost results for large battery combinations, which would be oversized in this application with the consequent lack of usage of the whole capacity. Therefore, these should not be contemplated for a ramp-rate control application from a financial point of view.

REFERENCES

[1] W. Jewell and R. Ramakumar, "The effects of moving clouds on electric utilities with dispersed photovoltaic generation," *IEEE Trans. Energy Convers.*, vol. EC-2, no. 4, pp. 570–576, Dec. 1987.

[2] G. Vahan and S. Booth, *Review of PREPA Technical Requirements for Interconnecting Wind and Solar Generation*. Golden, CO, USA: Nat. Renewable Energy Lab., 2013.

[3] H. E. State, "Hawaiian electric company state of the system summary for ESS RFP," Honolulu, HI, USA, 2014.

[4] J. Deign, "The faroe islands are getting Europe's first lithium-ion battery directly supporting wind," Green Tech Media, Boston, MA, USA, 2015. [Online]. Available: https://www.greentechmedia.com/articles/read/faroe-islands-support-wind-with-lithium-ion-battery

[5] M. J. E. Alam, K. M. Muttaqi, and D. Sutanto, "A novel approach for ramp-rate control of solar PV using energy storage to mitigate output fluctuations caused by cloud passing," *IEEE Trans. Energy Convers.*, vol. 29, no. 2, pp. 507–518, Jun. 2014.

[6] I. de la Parra, J. Marcos, M. García, and L. Marroyo, "Storage requirements for PV power ramp-rate control in a PV fleet," *Sol. Energy*, vol. 118, pp. 426–440, Aug. 2015.

[7] I. de la Parra, J. Marcos, M. García, and L. Marroyo, "Improvement of a control strategy for PV power ramp-rate limitation using the inverters: Reduction of the associated energy losses," *Sol. Energy*, vol. 127, pp. 262–268, 2016.

[8] X. Li, L. Yao, and D. Hui, "Optimal control and management of a large-scale battery energy storage system to mitigate fluctuation and intermittence of renewable generations," *J. Modern Power Syst. Clean Energy*, vol. 4, no. 4, pp. 593–603, 2016.

[9] A. Saez-de-Ibarra, E. Martinez-Laserna, D. I. Stroe, M. Swierczynski, and P. Rodriguez, "Sizing study of second life Li-ion batteries for enhancing renewable energy grid integration," *IEEE Trans. Ind. Appl.*, vol. 52, no. 6, pp. 4999–5008, Nov./Dec. 2016.

[10] J. Marcos, O. Storkël, L. Marroyo, M. Garcia, and E. Lorenzo, "Storage requirements for PV power ramp-rate control," *Sol. Energy*, vol. 99, pp. 28–35, Jan. 2014.

[11] N. Kakimoto, H. Satoh, S. Takayama, and K. Nakamura, "Ramp-rate control of photovoltaic generator with electric double-layer capacitor," *IEEE Trans. Energy Convers.*, vol. 24, no. 2, pp. 465–473, Jun. 2009.

[12] F. Diaz-Gonzalez, F. D. Bianchi, A. Sumper, and O. Gomis-Bellmunt, "Control of a flywheel energy storage system for power smoothing in wind power plants," *IEEE Trans. Energy Convers.*, vol. 29, no. 1, pp. 204–214, Mar. 2014.

[13] D. I. Stroe, A. I. Stan, R. Diosi, R. Teodorescu, and S. J. Andreasen, "Short term energy storage for grid support in wind power applications," in *Proc. Int. Conf. Optim. Elect. Electron. Equip.*, 2012, pp. 1012–1021.

[14] M. Świerczyński, D.-I. Stroe, A.-I. Stan, and R. Teodorescu, "Lifetime and economic analyses of lithium-ion batteries used for balancing the wind power forecast error: A case study for a single wind turbine," *Int. J. Energy Res.*, vol. 39, pp. 760–770, 2015.

[15] C. A. Hill, M. C. Such, D. Chen, J. Gonzalez, and W. M. K. Grady, "Battery energy storage for enabling integration of distributed solar power generation," *IEEE Trans. Smart Grid*, vol. 3, no. 2, pp. 850–857, Jun. 2012.

[16] J. Purewal, J. Wang, J. Graetz, S. Soukiazian, H. Tataria, and M. W. Verbrugge, "Degradation of lithium ion batteries employing graphite negatives and nickel-cobalt-manganese oxide + spinel manganese oxide positives: Part 2, chemical-mechanical degradation model," *J. Power Sources*, vol. 272, pp. 1154–1161, 2014.
[17] Y. Cui *et al.*, "Multi-stress factor model for cycle lifetime prediction of lithium ion batteries with shallow-depth discharge," *J. Power Sources*, vol. 279, pp. 123–132, 2015.
[18] D. Stroe, M. Swierczynski, A. Stan, and R. Teodorescu, "Accelerated lifetime testing methodology for lifetime estimation of lithium-ion batteries used in augmented wind power plants accelerate methodology for n of lithium-behave in used," *IEEE Trans. Ind. Appl.*, vol. 50, no. 6, pp. 4006–4017, Nov./Dec. 2014.
[19] M. Kassem, J. Bernard, R. Revel, S. Pélissier, F. Duclaud, and C. Delacourt, "Calendar aging of a graphite/LiFePO4cell," *J. Power Sources*, vol. 208, pp. 296–305, 2012.
[20] I. Bloom *et al.*, "An accelerated calendar and cycle life study of Li-ion cells," *J. Power Sources*, vol. 101, no. 2, pp. 238–247, 2001.
[21] Y. Wu, P. Keil, S. F. Schuster, and A. Jossen, "Impact of temperature and discharge rate on the aging of a $LiCoO_2$ /$LiNi_{0.8}$ $Co_{0.15}$ $Al_{0.05}$ O_2 Lithium-ion Pouch Cell," *J. Electrochem. Soc.*, vol. 164, no. 7, pp. A1438–A1445, 2017.
[22] V. Marano, S. Onori, Y. Guezennec, G. Rizzoni, and N. Madella, "Lithium-ion batteries life estimation for plug-in hybrid electric vehicles," in *Proc. Vehicle Power Propulsion Conf.*, 2009, pp. 536–543.
[23] M. Swierczynski, D. I. Stroe, A. I. Stan, R. Teodorescu, and D. U. Sauer, "Selection and performance-degradation modeling of LiMo2/Li4Ti5O12 and LiFePO4/C battery cells as suitable energy storage systems for grid integration with wind power plants: An example for the primary frequency regulation service," *IEEE Trans. Sustain. Energy*, vol. 5, no. 1, pp. 90–101, Jan. 2014.
[24] Y. Zhu, F. Yan, J. Kang, C. Du, C. Zhang, and R. F. Turkson, "Fading analysis of the Li(NiCoMn)O2battery under different SOC cycle intervals," *Ionics*, vol. 23, no. 6, pp. 1383–1390, 2017.
[25] J. de Hoog *et al.*, "Combined cycling and calendar capacity fade modeling of a nickel-manganese-cobalt oxide cell with real-life profile validation," *Appl. Energy*, vol. 200, pp. 47–61, 2017.
[26] J. Schmalstieg, S. Käbitz, M. Ecker, and D. U. Sauer, "A holistic aging model for Li(NiMnCo)O2 based 18650 lithium-ion batteries," *J. Power Sources*, vol. 257, pp. 325–334, 2014.
[27] I. Baghdadi, O. Briat, J. Y. Delétage, P. Gyan, and J. M. Vinassa, "Lithium battery aging model based on Dakin's degradation approach," *J. Power Sources*, vol. 325, pp. 273–285, 2016.
[28] I. de la Parra, J. Marcos, M. García, and L. Marroyo, "Control strategies to use the minimum energy storage requirement for PV power ramp-rate control," *Sol. Energy*, vol. 111, pp. 332–343, 2015.
[29] J. Sanchez, "Gestión de la Integración Eólica Masiva en Redes Eléctricas con Almacenamiento de Energía de Litio-Ion," in *Proc. IV Congreso Smart Grids*, 2017, pp. 1–6.
[30] H. Wenzl *et al.*, "Life prediction of batteries for selecting the technically most suitable and cost effective battery," *J. Power Sources*, vol. 144, no. 2, pp. 373–384, 2005.
[31] D. U. Sauer and H. Wenzl, "Comparison of different approaches for lifetime prediction of electrochemical systems—Using lead-acid batteries as example," *J. Power Sources*, vol. 176, no. 2, pp. 534–546, 2008.
[32] A. Barré, B. Deguilhem, S. Grolleau, M. Gérard, F. Suard, and D. Riu, "A review on lithium-ion battery ageing mechanisms and estimations for automotive applications," *J. Power Sources*, vol. 241, pp. 680–689, 2013.
[33] M. Berecibar, I. Gandiaga, I. Villarreal, N. Omar, J. van Mierlo, and P. van den Bossche, "Critical review of state of health estimation methods of Li-ion batteries for real applications," *Renewable Sustain. Energy Rev.*, vol. 56, pp. 572–587, 2016.
[34] J. Wang *et al.*, "Cycle-life model for graphite-LiFePO4cells," *J. Power Sources*, vol. 196, no. 8, pp. 3942–3948, 2011.
[35] D. I. Stroe, M. Swierczynski, A. I. Stan, V. Knap, R. Teodorescu, and S. J. Andreasen, "Diagnosis of lithium-ion batteries state-of-health based on electrochemical impedance spectroscopy technique," in *Proc. Energy Convers. Congr. Expo.*, 2014, pp. 4576–4582.
[36] T. Grün, K. Stella, and O. Wollersheim, "Impacts on load distribution and ageing in Lithium-ion home storage systems," *Energy Procedia*, vol. 135, pp. 236–248, 2017.
[37] S. Panchal *et al.*, "Cycling degradation testing and analysis of a LiFePO4 battery at actual conditions," *Int. J. Energy Res.*, vol. 41, no. 15, pp. 2565–2575, 2017.
[38] B. Weißhar and W. G. Bessler, "Model-based lifetime prediction of an LFP/graphite lithium-ion battery in a stationary photovoltaic battery system," *J. Energy Storage*, vol. 14, pp. 179–191, 2017.
[39] M. J. Swierczynski, "Lithium-ion battery energy storage system for augmented wind power plants," Ph.D. dissertation, Dept. Energy Technol., Aalborg Univ., Aalborg, Denmark, 2012.
[40] S. D. Downing and D. F. Socie, "Simple rainflow counting algorithms," *Int. J. Fatigue*, vol. 4, no. 1, pp. 31–40, 1982.
[41] E. Schaltz, A. Khaligh, and P. O. Rasmussen, "Influence of battery/ultracapacitor energy-storage sizing on battery lifetime in a fuel cell hybrid electric vehicle," *IEEE Trans. Veh. Technol.*, vol. 58, no. 8, pp. 3882–3891, Oct. 2009.
[42] H. Beltran, J. Barahona, R. Vidal, J. C. Alfonso, C. Ariño, and E. Pérez, "Ageing of different types of batteries when enabling a PV power plant to enter electricity markets," in *Proc. Annu. Conf. IEEE Ind. Electron. Soc.*, 2016, pp. 1986–1991.
[43] M. Safari, M. Morcrette, A. Teyssot, and C. Delacourt, "Life prediction methods for lithium-ion batteries derived from a fatigue approach," *J. Electrochem. Soc.*, vol. 157, no. 6, pp. 713–720, 2010.
[44] H. Beltran, M. Swierczynski, N. Aparicio, E. Belenguer, R. Teodorescu, and P. Rodriguez, "Lithium-ion batteries ageing analysis when used in a PV power plant," in *Proc. IEEE Int. Symp. Ind. Electron.*, 2012, pp. 1604–1609.
[45] J. Dambrowski, S. Pichlmaier, and A. Jossen, "Mathematical methods for classification of state-of-charge time series for cycle lifetime prediction," in *Proc. Adv. Automotive Battery Conf.*, 2012, vol. 2018, no. 15, pp. 2–4.
[46] C. M. Hoff and R. Lin, "Development and practical use of a levelized cost of storage (LCOS) metric," NEC Energy, Tokyo, Japan, 2016.
[47] C. S. Lai and M. D. McCulloch, "Levelized cost of energy for PV and grid scale energy storage systems," Sep. 2016. ArXiv preprint arXiv: 1609.06000.
[48] C. Pillot, "The rechargeable battery market and main trends 2016–2025," Avicenne Energy, Paris, France, 2017.
[49] C. Curry, "Lithium-ion battery costs and market," Bloomberg New Energy Finance, New York, NY, USA, 2017.
[50] IRENA, "Electricity storage and renewables: Costs and markets to 2030," Abu Dhabi, UAE, 2017.
[51] J. Mclaren, P. Gagnon, K. Anderson, E. Elgqvist, R. Fu, and T. Remo, "Battery energy storage market: Commercial scale, lithium-ion projects in the U.S.," Nat. Renewable Energy Lab., Golden, CO, USA, 2016.
[52] Lazard, "Lazard's levelized cost of storage analysis— Version 3.0," Hamilton, U.K., 2017.

Hector Beltran received the M.Sc. degree in industrial engineering from the Universitat Jaume I (UJI), Castelló de la Plana, Spain, in 2004, and the Ph.D. degree in electrical engineering from the Technical University of Catalonia (UPC), Barcelona, Spain, in 2011. Since 2006, he has been an Assistant Professor with the Electrical Engineering Area, UJI. His current research interests include massive PV integration into the grid and energy storage systems.

Iván Tomás García received the B.Sc. degree in industrial technology engineering, and the M.Sc. degree in industrial engineering, both from the UJI, in 2015 and 2017, respectively. He is currently working toward the master's degree in management, focused on innovation and internationalization, with UJI.

José Carlos Alfonso-Gil received the M.Sc. degree in automation and industrial electronics engineering from Universitat Politècnica de València (UPV), València, Spain, in 2004, and the Ph.D. degree in electronics engineering in 2010. Since 2007, he has been an Assistant Professor with the Electrical Engineering Area, at UJI. His fields of interest are active power filters, control of power converters, and microgrids.

Emilio Pérez received the M.Sc. degree in industrial engineering from UJI, in 2002, and the Ph.D. degree in control engineering from UPV, in 2011. Since 2006, he has been with the Electrical Engineering Area, UJI, where he is currently an Assistant Professor. His current research interests include control and optimization of PV systems with energy storage, solar forecasting, and lithium-ion batteries, ageing and management.

Levelized Cost of Storage for Li-Ion Batteries Used in PV Power Plants for Ramp-Rate Control

Hector Beltran, Iván Tomás García, José Carlos Alfonso-Gil, and Emilio Pérez

***Abstract*—Photovoltaic (PV) power production ramp-rate control is getting more and more important in weak electric power systems, in which quick and significant power fluctuations can affect the stability of the system. This can be achieved by means of the integration of batteries into large PV plants but such an operation involves an aggressive environment for the ageing of the batteries. This paper presents an evaluation of this ageing by means of the annual simulations of a large PV power plant using actual irradiance data. This is done for different battery sizes used under various degrees of limitation in the power ramp-rate variation. The levelized cost of storage is calculated for each of the cases considered.**

***Index Terms*—Photovoltaic power plants with energy storage, ramp-rate control, batteries, ageing analysis.**

I. Introduction

The power fluctuations experienced by Photovoltaic (PV) power plants as a consequence of the low, fast-moving clouds over them is one of the most important challenges for the massive integration of this technology in the electric power system. Since clouds' impacts are highly localized effects, this handicap has been typically minimized thanks to the general dispersion of PV generators in a wide area region [1]. However, the growing development and penetration of large scale PV installations in weak or isolated power grids is posing new challenges for the corresponding electric power system operators. The challenges are mainly associated to the grid stability because these systems are usually not very vast. Then, when a significant part of the energy production is highly variable, the system operators have to define or impose certain restrictions to the stochasticity of the PV production. This is being faced by certain operators such as the Puerto Rico Electric Power Authority (PREPA, [2]), the Hawaiian Electric Company (HECO, [3]), or the Faroe Islands utility (SEV, [4]) all of them good examples of weak grids. The solution being defined is based in the introduction of certain ramp-rate power limitations that restrict the variation of the PV production over short-periods of time. This can be achieved with the integration in the PV power plants of some type of energy storage system, mainly batteries, Fig. 1. Various proposals are available in the literature that analyze their use under this ramp-rate power control strategy [5]–[10], and even the use of ultracapacitors for it [11]. Similar proposals are done by other authors for wind power plants with storage [12]–[15].

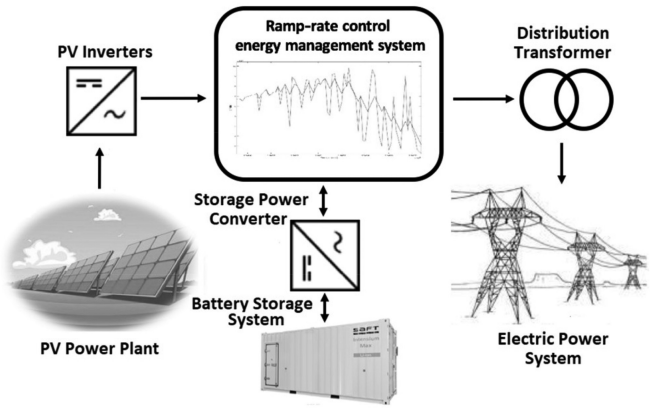

Fig. 1. Scheme of the PV plant with batteries for power ramp-rate control.

Therefore, it is the role of the energy storage system (batteries) operating within the renewable energy source power plant to cope with the power difference during the periods in which the PV panels have stochastically and rapidly varied their production and must inject into the grid a given limited production while the PV panels produce differently. In this way, the ramp-rate control achieved thanks to the introduction of batteries in a renewable energy power plant implies a more or less continuous mode of operation in which the batteries are being charged and discharged over and over. This involves ageing the batteries accordingly. Multiple authors have analyzed the ageing mechanisms associated to the batteries under different stress factors [16]–[21], and propose different types of models to evaluate it and perform some type of prognosis [22]–[27].

Although different authors have faced the PV power ramp-rate control strategy using batteries, it is important to highlight that these mainly focus on the definition of new control algorithms that usually pursue either the minimization of the size of the batteries (energy capacity requirements) or the optimized operation of the PV plant with storage. Moreover, the references cited for battery ageing are mainly associated to the electric vehicle industry. Therefore, none of the previous works has investigated the impact on the ageing of the batteries produced by the power ramp-rate limitation strategy when implemented in a PV power plant. This work presents such an evaluation by

Manuscript received March 29, 2018; revised October 23, 2018; accepted December 20, 2018. This work was supported by Universitat Jaume I through its special program to foster the scientific research and the technological development under Grant UJI-B2017-26. Paper no. TEC-00322-2018. *(Corresponding author: Hector Beltran.)*

The authors are with the Department of Industrial Systems Engineering and Design, Universitat Jaume I, Castelló de la Plana 12071, Spain (e-mail: hbeltran@uji.es; al190105@uji.es; jalfonso@uji.es; pereze@uji.es).

Color versions of one or more of the figures in this paper are available online at http://ieeexplore.ieee.org.

Digital Object Identifier 10.1109/TEC.2019.2891851

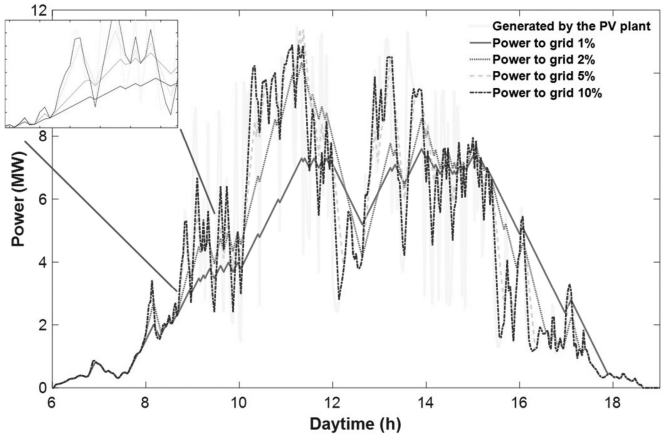

Fig. 2. Power production of the 10 MW PV plant with batteries under different degrees of ramp-rate limitation (defined in % in the legend).

means of annual simulations of a large PV power plant (10 MW) using actual irradiance data. This is done for different sizes of batteries used under various degrees of limitation in the power ramp-rate variation. The Levelized Cost of Storage (LCOS) is calculated for each of the combinations.

Then, after discussing about the potential type of Li-ion battery to be used in such an application in Section II, and the stress factors that can affect their lifetime in Section III, the current work analyzes in Sections IV and V the ageing experienced by the batteries taking into account both calendar and cycle ageing models. The paper concludes with the estimation of the LCOS and some final remarks.

II. PV Power Ramp-Rate Control With Batteries

Due to the inherent fluctuation of the PV power production associated to the transient clouds, which can achieve values beyond 90% and 70% for 1 MW and 10 MW PV plants in one single minute, respectively [28], some electric system operators controlling weak power grids are starting to impose some limitations to the production variability of this renewable technology. As already introduced in the previous section, this is a well stablished and known control proposal defined in various electric codes and implemented in actual systems to avoid stability problems. Also in the literature, different authors have analyzed this solution for PV plants and defined some variations intended to: minimize the size of the batteries involved [6], [7], [10], [28], to perform some supervisory control over the operation of the combined "PV + storage" plants [8], or to optimize the size of the potential second-life batteries to be used with this goal [9].

We analyze in our work four different degrees of power ramp-rate variation, the cases in which the PV power plant production with batteries is allowed to modify its production every minute no more than 1%, 2%, 5%, and 10%, with regard to its PV rated power, Fig. 2. These limitation levels correspond to the usual control levels defined in the grid codes that already demand it (mostly 10%) and to potential more restrictive levels ($<$10%) to be fixed in the coming future. In this sense, the lower the power variation allowed (in %), the higher the degree of filtering introduced by the batteries and, accordingly, the deeper the charge-and-discharge cycling pattern experienced with the consequent ageing. The depth-of-discharge of the cycles will be also function of the battery energy capacity, which will be analyzed in between 1 and 10 MWh for the 10 MW rated power PV plant under consideration. These energy capacity values are based on the characteristics of the existing installations.

Regarding the type of batteries, up to six different families are commercialized nowadays: Lithium Cobalt Oxide (LCO or LiCoO2), Lithium Iron Phosphate (LFP or LiFePO4), Lithium Nickel Cobalt Aluminium Oxide (NCA or LiNiCoAlO2), Lithium Manganese Oxide (LMO or LiMn2O4), Lithium Nickel Manganese Cobalt Oxide (NMC or LiNiMnCoO2), and Lithium Titanate (LTO or Li4Ti5O12). These mainly differ in the material constituting the cathode. Only the LTO family associates its name to the anode's material, being in all the cases the second electrode made of graphite. The operational characteristics also differ being NCA the one with highest specific energy; however, LFP and LTO are superior in terms of specific power, cyclability, and thermal stability, what makes them appropriate for intensive power demanding applications such as ramp-rate control. LTO also presents the best life span although it is the most expensive technology. In all, since space is not a limiting parameter for this type of installation and price is lower than for other lithium types, LFP is the selected chemistry for our analysis. Note in this regard that it is being developed and installed by companies such as SAFT Batteries for ramp-rate control applications in wind farms [29].

III. Battery Ageing Stress Factors and Model

The ageing phenomenon of Li-ion based batteries has been extensively analyzed in the literature in the last years due to its importance not only for the renewables' integration expansion but mainly for the electric vehicle continuously increasing industry. In this sense, the multiple ageing models and analyses performed have been classified by different authors [30]–[33] into 2 main groups: performance-based lifetime models, and post-processing models. The way to analyse the ageing differs in the different works, however, the resulting stress factors are quite coherent among publications for the various battery chemistries analysed.

A. Battery Ageing Stress Factors

The identified stress factors that influence the ageing of Li-ion batteries can be mainly listed as: time, temperature, state-of-charge (SOC) during rest, number of cycles experienced, depth-of-discharge (DoD) of the cycles, average voltage of the cycles, and charge/discharge current rate.

Their corresponding influence depends on the type of battery and on the design under consideration and is usually studied according to two types of mechanism: calendar and cycle ageing. Then, while the calendar ageing is usually associated to the capacity reduction of the batteries as a function of time without being cycled (only by being connected in hot stand-by), the cycle ageing is associated to their continuous use (by being charged and discharged). In this sense and for the case of Li-ion

batteries, the calendar ageing gets generally more significant with time as temperature and SOC are higher [16]–[20]. The relation with temperature is normally modelled by means of the Arrhenius equation (1) while the dependence over the voltage (or SOC) is generally less important and follows a polynomial or even linear relation, depending on the lithium battery type.

$$k\left(t\right) = A \times e^{-\frac{Ea}{RT}} \tag{1}$$

With regard to the cycle ageing, this is highly influenced by the number of cycles experienced [22]. The DoD of the cycles is also important, having a lower ageing effect with shallower depth cycles [17], [22], as it is important to perform the cycles as close as possible to the 50% of SOC to minimize the ageing impact due to the average voltage during the cycling [18], [23]–[26]. Finally, also the temperature significantly affects the cycle ageing [21], [25]–[27] what forces most battery manufacturers to advice their use under refrigerated conditions not much above 25 °C. After all, it can be concluded that both effects (calendar and cycle) are important and dependent on the combination and degree of the stress factors [16]. Therefore, none of them can be disregarded in a thorough full research.

B. Ageing Model Used for Analysis

As discussed previously, due to the application under study (power rate-ramp control for a large PV plant), the use of LFP batteries is analysed. Therefore, among the multiple Li-ion equivalent model proposals, only some of those focused on this chemistry have been considered in depth [18], [19], [23], [25], [34]–[38]. And among them, since some have been developed based on electric vehicle (EV) standard drive cycle profiles, only those from Stroe [18], Swierczynski [23], and Weißhar [38] are considered appropriate for our analysis. These authors propose different ageing models for LFP batteries combined with renewable energy plants. However, the latter applies them for small domestic installations. Therefore, due to the similarity with the type of application analysed in Stroe [18] for wind power plants, the present work uses the model proposed by this author to analyse how LFP batteries are going to lose capacity over time when used for power rate-ramp control in a large PV plant. This model is based on the following semi-empirical equations defined for both capacity fades (in %) associated respectively to the calendar and the cycle ageing:

$$C_{fade,cal}\left(t,T\right) = \alpha_t \times e^{\beta_t \cdot T} \times t^n \tag{2}$$

$$C_{fade,cyc}\left(NC,T\right) = \alpha_{NC} \times e^{\beta_{NC} \cdot T} \times NC^n \tag{3}$$

Where *t* is the time in months, *T* is the temperature in Kelvin, and *NC* represents the number of equivalent reference cycles. The coefficients in these equations are $\alpha_t = 3.087 \cdot 10^{-7}$, $\alpha_{NC} = 6.87 \cdot 10^{-5}$, $\beta_t = 0.05146$, $\beta_{NC} = 0.027$, and n = 0.5, for both equations. Note that the C-rate stress factor influence is not included in the model because C-rates below 4C are considered in the application analysed in our work. Under these operating conditions, the C-rate influence can be neglected [39].

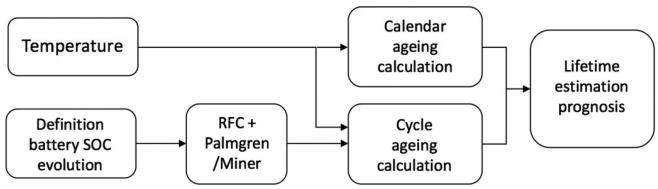

Fig. 3. Structure of the methodology implemented to analyze the LFP battery capacity fade along the ramp-rate control operation.

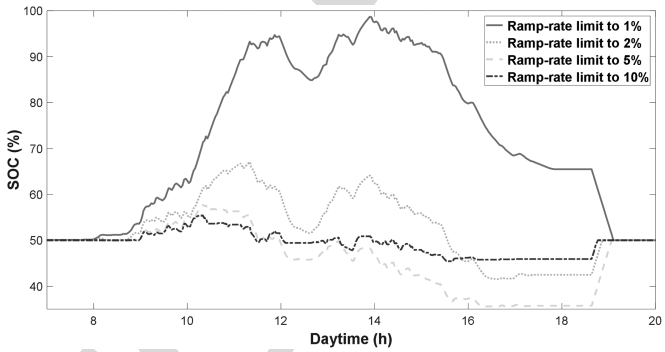

Fig. 4. State-of-charge evolution of the 5 MW battery under different degrees of ramp-rate limitation for the day represented in Fig. 2.

IV. Analysis of the Ageing Under Ramp-Rate Control

This analysis is based on the ageing model introduced in the previous section which is combined in this work with the rainflow-counting (RFC) algorithm [40]–[42] and the Palmgren-Miner rule [22], [43]–[45]. In this way, the proposed hybrid methodology provides an estimation of the lifetime expectancy of the batteries under the power ramp-rate control regime of operation.

A. Methodology Implemented for the Ageing Prognosis

The methodology developed to analyze the ageing is summarized in Fig. 3, where the scheme interrelating the inputs, the calculation/simulation steps, and the final output is shown.

Then, the proposed analysis model presents various stages that can be clearly observed. First, the evolution of the SOC of the battery experienced along one whole year operating under the ramp-rate control regime is generated. As can be observed in Fig. 4 for the day whose power exchanges are represented in Fig. 2, this is done for four different degrees of ramp rate control limitation (1%/min, 2%/min, 5%/min, and 10%/min), introducing in all the cases a programmed SOC recovery of its initial value (50%) after the battery daily operation.

The analysis in this work is also performed for various battery sizes (from 1 MWh up to 10 MWh), for two extreme potential roundtrip efficiencies of the batteries (85%, and 92%), and for two different operating temperatures (25 °C and 35 °C), at which the batteries are considered to be refrigerated on-site. The battery exchange power capacity is always considered the same and defined as 5 MW, according to recommendations from SAFT for this specific application.

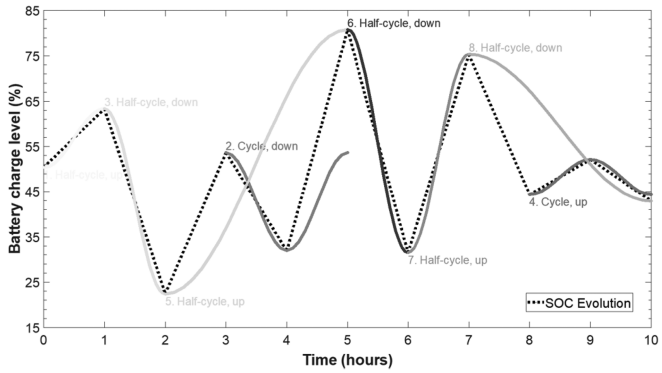

Fig. 5. Adaptation performed by the RFC MATLAB function to the SOC evolution to account the number of half cycles and their DoD.

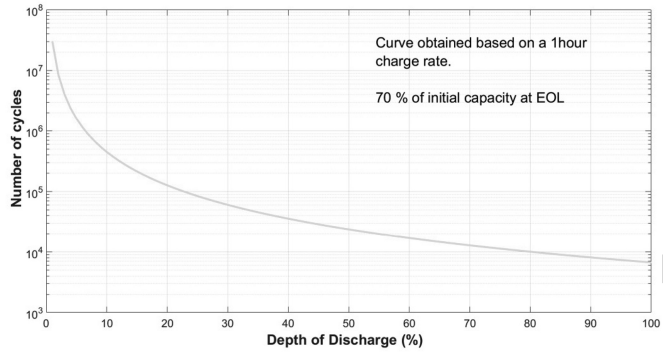

Fig. 6. Cycles to failure vs. DoD curve for LFP batteries from SAFT.

Then, following the scheme, the SOC evolution curve is introduced into the RFC algorithm which processes the SOC curve as represented in Fig. 5. This returns the number of cycles experienced by the battery at varying DoDs, as well as the medium voltage for each partial charge/discharge cycle.

This information is then handled by the Palmgren-Miner rule (4) which compares the partial cycling histogram provided by the RFC with the maximum number of cycles that the battery could perform at each single DoD. This equation dispenses the degradation (*D*) experienced over the simulated time period:

$$D(\%) = \sum_{DoD=1}^{DoD=100} \frac{N_{cyc}\,(DoD)}{N_{\max}\,(DoD)} \tag{4}$$

Where N_{cyc} is the number of cycles returned by the RFC algorithm and experienced for each amplitude (defined by the *DoD* variable), and $N_{\max}$ is the number of cycles the battery can withstand for each specific DoD, according to the capacity evolution curves of the batteries provided by the manufacturer. Fig. 6 plots this curve for the case of the Intensium Max High Power VL30P cells type from SAFT batteries, which can be approximated by the following equation (5):

$$N_{\max}\,(\mathrm{DoD}) = 3 \cdot 10^7 \times DoD(\%)^{-1.825} \tag{5}$$

The degradation parameter D calculated in (4) is useful to estimate the number of equivalent reference cycles (*NC*) that the battery has experienced over the year. As deduced from

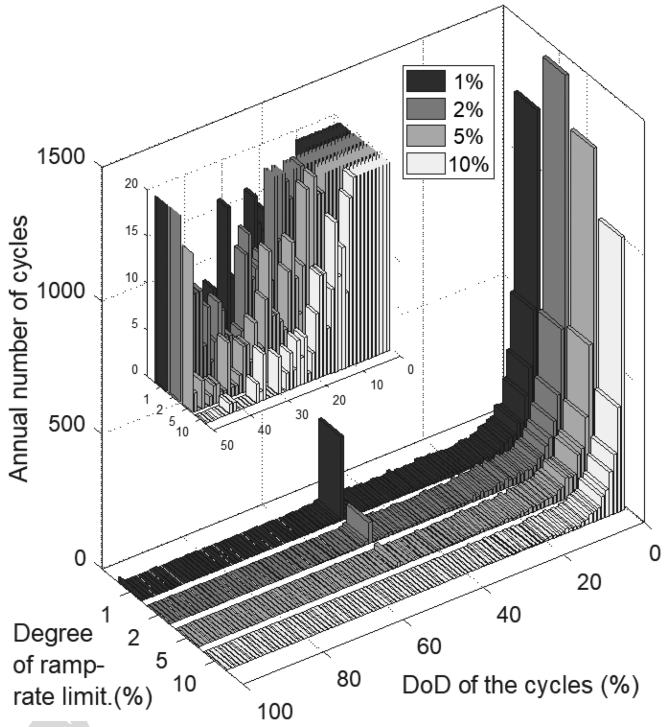

Fig. 7. Histograms representing the annual cycling pattern of a 5 MW / 5 MWh battery under the four different degrees of ramp-rate limitation, with a zoom over the range 0–50% in DoD of the cycles and up to 20 accumulated cycles.

Fig. 6, these LFP batteries can withstand around 10000 cycles at 80% DoD, what means that the *NC* can be calculated as (6).

$$NC\,(@80\%) = \frac{D\,(\%) \times 10000}{100\%} \tag{6}$$

Thereafter, once accounted the *NC*, this information is introduced into equations (2) and (3) together with the temperature. The resulting capacity fade values are combined to finally provide the lifetime estimation prognosis, in years, by means of equation (7) which takes into account that the battery manufacturer defines the end-of-life (EOL) of the batteries when the retained capacity (*RC*) is the 70% of its initial value.

$$RC = \{1 - [C_{fade,cal}\,(y_{EOL}, T) + C_{fade,cyc}\,(NC, T) \times y_{EOL}]\} \tag{7}$$

The solution in years (y_{EOL}) at this equation is the estimated lifetime of the battery (EOL time). All the procedure has been implemented and automated in Matlab/Simulink which presents a RFC library that simplifies part of the programming.

B. Results of the Ageing Analysis

Annual simulations of a 10 MW PV power plant using actual irradiance data have been performed to avoid seasonal effects for all the cases described in the previous sections (different filtering levels, various battery energy capacity sizes, and two operating temperatures). The simulations have been done with a one-minute time step, what provides a good track of the fast power fluctuations. Then, the obtained SOC evolution of the various batteries were treated with the RFC algorithm to derive the cycling histograms as the one represented in Fig. 7.

TABLE I
LIFETIME ESTIMATION (IN YEARS) FOR A ROUNDTRIP EFF. = 85%

Temp = 25ºC

Capacity \ Filt.	1%	2%	5%	10%
1 MWh	3.18	3.38	4.22	5.42
2 MWh	3.98	4.26	5.62	7.69
3 MWh	4.22	5.01	6.89	9.42
4 MWh	4.59	5.48	8.00	11.2
5 MWh	4.98	6.08	8.98	12.6
6 MWh	5.08	6.65	9.75	14.0
7 MWh	5.32	7.12	10.6	15.1
8 MWh	5.72	7.70	11.4	16.1
9 MWh	6.02	8.20	12.2	17.0
10 MWh	6.23	8.70	13.0	17.7

Temp = 35ºC

Capacity \ Filt.	1%	2%	5%	10%
1 MWh	2.06	2.15	2.65	3.30
2 MWh	2.35	2.70	3.34	4.36
3 MWh	2.69	3.05	4.04	5.28
4 MWh	2.92	3.30	4.48	6.07
5 MWh	3.02	3.66	5.05	6.65
6 MWh	3.09	4.00	5.35	7.17
7 MWh	3.24	4.18	5.85	7.57
8 MWh	3.38	4.38	6.18	8.01
9 MWh	3.59	4.71	6.42	8.26
10 MWh	3.79	5.01	6.82	8.50

TABLE II
LIFETIME ESTIMATION (IN YEARS) FOR A ROUNDTRIP EFF. = 92%

Temp = 25ºC

Capacity \ Filt.	1%	2%	5%	10%
1 MWh	3.15	3.35	4.12	5.35
2 MWh	3.92	4.20	5.44	7.42
3 MWh	4.16	5.00	6.68	9.28
4 MWh	4.50	5.38	7.76	11.0
5 MWh	4.89	6.01	8.67	12.3
6 MWh	5.05	6.42	9.42	13.6
7 MWh	5.26	7.05	10.3	14.8
8 MWh	5.59	7.44	11.2	15.7
9 MWh	6.00	8.05	12.0	16.6
10 MWh	6.11	8.41	12.7	17.4

Temp = 35ºC

Capacity \ Filt.	1%	2%	5%	10%
1 MWh	2.05	2.11	2.58	3.27
2 MWh	2.34	2.67	3.29	4.32
3 MWh	2.66	3.02	4.01	5.23
4 MWh	2.89	3.27	4.38	6.01
5 MWh	3.01	3.58	5.00	6.50
6 MWh	3.07	3.95	5.28	7.08
7 MWh	3.20	4.10	5.70	7.42
8 MWh	3.33	4.32	6.08	7.88
9 MWh	3.50	4.59	6.34	8.17
10 MWh	3.71	4.91	6.67	8.38

By applying the rest of the analysis methodology to these histograms, the ageing prognosis for the multiple case studies is obtained. The resulting lifetime estimation to achieve the 30% drop in energy capacity is summarized in Table I and Table II, for the roundtrip efficiencies of 85% and 92%, respectively, and for the two temperatures considered.

Results indicate that improving the roundtrip efficiency of the battery from 85% up to 92% on the AC side of the energy storage system has not significant effect to the battery ageing. On the contrary, operating the battery at 35 °C instead of 25 °C represents a potential life span reduction varying from 40% to 60%. Therefore, it is clear that the operation temperature of the battery cells should be kept under control and as close as possible to the 20–25 °C recommended by manufacturers. Although not summarized on these tables, further simulations performed for 20 °C confirm lifetime can be further extended by another 20–25% at this temperature. With regard to the degree of control of the ramp-rate variations, it stands out how the more restrictive the control is (lower percentage of variation allowed) the shorter the lifetime expectancy because the battery is more demanded. Finally, note how, similarly, the increasing energy capacity of the battery favors the extension of its lifetime due to the shallower cycles experienced throughout the annual operation for a given power exchange pattern with the grid.

Further conclusions can be obtained from the graphical representation in Fig. 8. This shows for different operation conditions the capacity fades associated to the calendar (red) and to the cycling (blue) ageing mechanisms, which add up the 30% fade of the initial battery capacity accepted by the manufacturer as EOL (70% of capacity retention). Although the cycle ageing is generally assumed to be more important than the calendar one, it is straightforward derived from Fig. 8 that both types of ageing mechanisms are significant and both have to be taken into consideration in this application for the design and sizing definition of the battery to guarantee a proper lifetime. Note how their corresponding weight on the overall ageing of the battery is clearly dependent on the battery size and on the filtering level, since these two design parameters condition the DoD of the cycles experienced during the annual operation. It is therefore important to highlight that histogram results in Fig. 7 together with the surfaces represented in Fig. 8 demonstrate that the ramp-rate control strategy analyzed in this work is not a very demanding energy management strategy for batteries used in a PV power plant from a cycle ageing mechanism point of view. Clearly, the calendar ageing is also significant in this application and cannot be despised. Finally, note that the progressive reduction of the battery capacity with time and use will imply a lower and lower capability to control the ramp-rate as the EOL of the battery approaches.

V. ESTIMATION OF THE LEVELIZED COST OF STORAGE

Once the ageing of the batteries has been quantified, it is necessary to identify a valid method to define or calculate the relative and comparable costs of the different battery solutions analyzed to provide the ramp-rate control service. Energy storage systems that are implemented as a way to improve the management capability and the quality of the energy discharged to the grid pose a complex problem to quantify its benefits and effectiveness with respect to their cost. This is due to the fact that they do not produce electricity from an energy source, but store it for a time, and to the interrelation that exists among all the aspects that take part in their operation. All of this makes the evaluation difficult with a simple analysis.

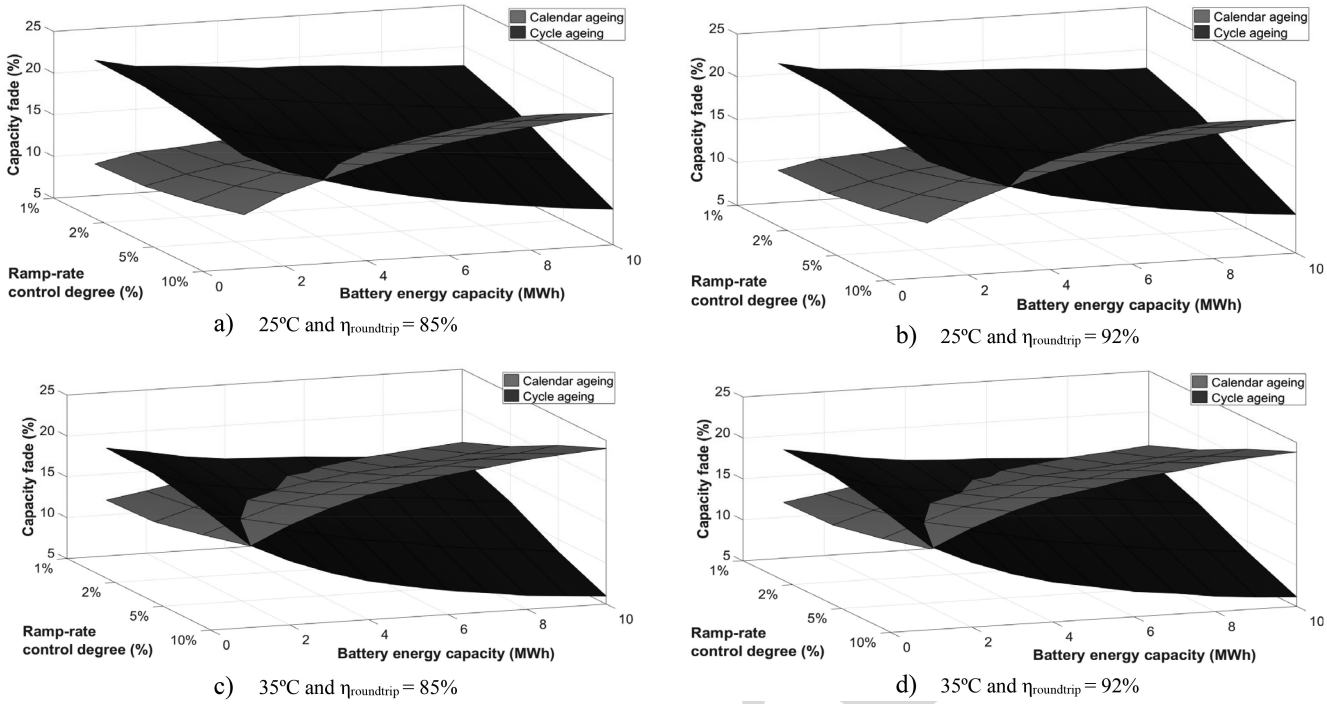

Fig. 8. Capacity loss (in %) experienced by a 5 MW battery at 25 °C [a) and b)] and 35 °C [c) and d)] for the two roundtrip efficiencies under consideration.

Levelized Cost of Storage (LCOS) is an innovative tool [46] derived from the traditional LCOE calculation [47], used to compare the lifetime cost of the energy producing technologies, but adapted to energy storage systems that do not produce energy by themselves but store it for a later use introducing some energy losses. Therefore, LCOS is being used to compare the cost of using different storage technologies along their lifespan for a given application in the electric power sector. In this sense, LCOS can be defined as the cost per usable energy storage capacity throughout the lifetime of the installation. This is calculated, according to [46], taking into account the initial investment of the system, plus all the operating and maintenance costs accumulated during its use, divided by the so-called lifetime utilization factor (LUF), as in (8):

$$LCOS_{EOL} = \frac{I_o + \sum_{y=0}^{EOL} Op_{cost}}{\sum_{y=0}^{EOL} C_y \times \sqrt{\eta_y} \cdot \Delta t} \ (€/\text{kWh per year}) \quad (8)$$

Where the different parameters involved are:

- *EOL*, lifetime expectancy in years, according to the analysis introduced in the previous section.
- I_o, initial investment cost of the whole energy storage system (batteries, converters, cooling unit, protections and control equipment . . .), in €/kWh.
- Op_{cost}, overall operating annual cost (maintenance, security, recharge costs, auxiliary power, control and management). This is usually accounted for as a percentage of the initial investment, also in €/kWh.
- C_y, energy capacity of the battery let at year "y" with regard to its initial value (100%-degradation), in %.
- η_y, battery roundtrip AC-to-AC efficiency, in %.
- Δt, the incremental time, in years.

TABLE III
INITIAL INVESTMENT COST OF THE 5 MW BATTERIES (IN M€) FOR THE DIFFERENT BATTERY CAPACITIES TAKEN INTO ACCOUNT

1 MWh	2 MWh	3 MWh	4 MWh	5 MWh
1.45	1.9	2.35	2.8	3.25
6 MWh	7 MWh	8 MWh	9 MWh	10 MWh
3.27	4.15	4.6	5.05	5.5

For this calculation, the initial investment cost has been introduced according to that in Table III for the different battery energy capacities. These costs are based on the average price per kW and kWh of installed LFP battery (including all the equipment) registered and estimated in various reports from different international technology centers and specialized consultancies [48]–[51]. The overall operating annual costs has been assumed to be the 3.5% of the initial investment, upon estimations from battery manufacturers. An annual monetary discount rate equal to 4% is also assumed. The annual capacity left in the battery is updated every year as a function of the calculated degradation parameter. As it is done with the one-way efficiency which is initially taken as 96% (corresponding to the roundtrip efficiency of 92% previously analyzed). The case of the 85% roundtrip efficiency has not been calculated due to the low impact reflected on the ageing that has been already discussed.

Therefore, according to (8) and taking into account the ageing results and estimated lifetimes presented before, Table IV summarizes the LCOS calculated values at the EOL of the batteries for the different combinations of parameters that have been considered at both 25 °C and 35 °C. It is notably remarkable

TABLE IV
LCOS OF THE 5 MW BATTERIES BASED ON THE ESTIMATED EOL (IN €/KWH)

Temp = 25ºC

Capacity \ Filt.	1%	2%	5%	10%
1 MWh	665	630	512	403
2 MWh	352	330	261	197
3 MWh	275	230	179	134
4 MWh	229	194	140	111
5 MWh	196	162	118	88
6 MWh	180	146	104	77
7 MWh	167	128	96	69
8 MWh	154	119	84	64
9 MWh	140	108	78	59
10 MWh	135	102	73	56

Temp = 35ºC

Capacity \ Filt.	1%	2%	5%	10%
1 MWh	1020	997	785	644
2 MWh	597	523	420	394
3 MWh	433	372	283	222
4 MWh	350	311	235	174
5 MWh	309	265	191	152
6 MWh	289	227	174	133
7 MWh	268	210	156	124
8 MWh	251	195	142	113
9 MWh	234	180	134	107
10 MWh	216	165	126	103

from the results that although the initial investment cost obviously influences the LCOS value of the system, the increase in the estimated service life of the batteries, due to a less stressing operation regime and the consequent reduced ageing, involves a decrease in the resulting LCOS of the larger energy capacity batteries. Therefore, the larger the capacity, the lower the LCOS in this application. Still, the operating temperature is also very important since the LCOS can vary for the same battery and ramp-rate limitation level between 40 and 50% for operating temperatures going from 25 °C up to 35 °C.

Finally, note that results presented in this work can be compared with those provided by the financial advisory and asset management firm Lazard in [52]. This consultancy offers LCOS values ranging from $272 up to $386 for "in-front-of-the-meter" applications. Therefore, some of the combinations analyzed here offer a LCOS quite lower than those estimated by Lazard. However, this is mainly obtained for large capacity batteries that, although taken into account here, would be difficult to justify for the ramp-rate control application from an economic and financial point of view.

VI. CONCLUSIONS

In conclusion, the ramp-rate PV power production control is a grid injection power limitation that is gaining importance in the electric systems, mainly in weak power systems to the moment, as the degree of penetration of PV power plants gets higher. The inherently intermittent and stochastic power production fluctuations of this technology could affect the stability of the system. This limitation can be managed by integrating batteries into large PV plants but such an operation involves an aggressive environment for the ageing of the batteries. This work has analyzed this ageing for a specific technology of lithium ion batteries, the LFP family. Results in this sense highlight the importance of the temperature of operation of the batteries as well as the influence of the battery size and degree of ramp-rate limitation on the cycle ageing. Lifetime estimations range from 3.6 years up to 12.2 years depending on the battery size and the ramp-rate control at 35 °C. This ageing prognosis opened the door to a careful analysis of the Levelized Cost of Storage for this application using batteries. In this sense, LCOS results are in accordance with previous reports and tend to offer optimistic low cost results for large battery combinations, which would be oversized in this application with the consequent lack of usage of the whole capacity. Therefore, these should not be contemplated for a ramp-rate control application from a financial point of view.

REFERENCES

[1] W. Jewell and R. Ramakumar, "The effects of moving clouds on electric utilities with dispersed photovoltaic generation," *IEEE Trans. Energy Convers.*, vol. EC-2, no. 4, pp. 570–576, Dec. 1987.

[2] G. Vahan and S. Booth, *Review of PREPA Technical Requirements for Interconnecting Wind and Solar Generation*. Golden, CO, USA: Nat. Renewable Energy Lab., 2013.

[3] H. E. State, "Hawaiian electric company state of the system summary for ESS RFP," Honolulu, HI, USA, 2014.

[4] J. Deign, "The faroe islands are getting Europe's first lithium-ion battery directly supporting wind," Green Tech Media, Boston, MA, USA, 2015. [Online]. Available: https://www.greentechmedia.com/articles/read/faroe-islands-support-wind-with-lithium-ion-battery

[5] M. J. E. Alam, K. M. Muttaqi, and D. Sutanto, "A novel approach for ramp-rate control of solar PV using energy storage to mitigate output fluctuations caused by cloud passing," *IEEE Trans. Energy Convers.*, vol. 29, no. 2, pp. 507–518, Jun. 2014.

[6] I. de la Parra, J. Marcos, M. García, and L. Marroyo, "Storage requirements for PV power ramp-rate control in a PV fleet," *Sol. Energy*, vol. 118, pp. 426–440, Aug. 2015.

[7] I. de la Parra, J. Marcos, M. García, and L. Marroyo, "Improvement of a control strategy for PV power ramp-rate limitation using the inverters: Reduction of the associated energy losses," *Sol. Energy*, vol. 127, pp. 262–268, 2016.

[8] X. Li, L. Yao, and D. Hui, "Optimal control and management of a large-scale battery energy storage system to mitigate fluctuation and intermittence of renewable generations," *J. Modern Power Syst. Clean Energy*, vol. 4, no. 4, pp. 593–603, 2016.

[9] A. Saez-de-Ibarra, E. Martinez-Laserna, D. I. Stroe, M. Swierczynski, and P. Rodriguez, "Sizing study of second life Li-ion batteries for enhancing renewable energy grid integration," *IEEE Trans. Ind. Appl.*, vol. 52, no. 6, pp. 4999–5008, Nov./Dec. 2016.

[10] J. Marcos, O. Storkël, L. Marroyo, M. Garcia, and E. Lorenzo, "Storage requirements for PV power ramp-rate control," *Sol. Energy*, vol. 99, pp. 28–35, Jan. 2014.

[11] N. Kakimoto, H. Satoh, S. Takayama, and K. Nakamura, "Ramp-rate control of photovoltaic generator with electric double-layer capacitor," *IEEE Trans. Energy Convers.*, vol. 24, no. 2, pp. 465–473, Jun. 2009.

[12] F. Diaz-Gonzalez, F. D. Bianchi, A. Sumper, and O. Gomis-Bellmunt, "Control of a flywheel energy storage system for power smoothing in wind power plants," *IEEE Trans. Energy Convers.*, vol. 29, no. 1, pp. 204–214, Mar. 2014.

[13] D. I. Stroe, A. I. Stan, R. Diosi, R. Teodorescu, and S. J. Andreasen, "Short term energy storage for grid support in wind power applications," in *Proc. Int. Conf. Optim. Elect. Electron. Equip.*, 2012, pp. 1012–1021.

[14] M. Świerczyński, D.-I. Stroe, A.-I. Stan, and R. Teodorescu, "Lifetime and economic analyses of lithium-ion batteries used for balancing the wind power forecast error: A case study for a single wind turbine," *Int. J. Energy Res.*, vol. 39, pp. 760–770, 2015.

[15] C. A. Hill, M. C. Such, D. Chen, J. Gonzalez, and W. M. K. Grady, "Battery energy storage for enabling integration of distributed solar power generation," *IEEE Trans. Smart Grid*, vol. 3, no. 2, pp. 850–857, Jun. 2012.

[16] J. Purewal, J. Wang, J. Graetz, S. Soukiazian, H. Tataria, and M. W. Verbrugge, "Degradation of lithium ion batteries employing graphite negatives and nickel-cobalt-manganese oxide + spinel manganese oxide positives: Part 2, chemical-mechanical degradation model," *J. Power Sources*, vol. 272, pp. 1154–1161, 2014.
[17] Y. Cui *et al.*, "Multi-stress factor model for cycle lifetime prediction of lithium ion batteries with shallow-depth discharge," *J. Power Sources*, vol. 279, pp. 123–132, 2015.
[18] D. Stroe, M. Swierczynski, A. Stan, and R. Teodorescu, "Accelerated lifetime testing methodology for lifetime estimation of lithium-ion batteries used in augmented wind power plants accelerate methodology for n of lithium-behave in used," *IEEE Trans. Ind. Appl.*, vol. 50, no. 6, pp. 4006–4017, Nov./Dec. 2014.
[19] M. Kassem, J. Bernard, R. Revel, S. Pélissier, F. Duclaud, and C. Delacourt, "Calendar aging of a graphite/LiFePO4cell," *J. Power Sources*, vol. 208, pp. 296–305, 2012.
[20] I. Bloom *et al.*, "An accelerated calendar and cycle life study of Li-ion cells," *J. Power Sources*, vol. 101, no. 2, pp. 238–247, 2001.
[21] Y. Wu, P. Keil, S. F. Schuster, and A. Jossen, "Impact of temperature and discharge rate on the aging of a $LiCoO_2$ /$LiNi_{0.8}$ $Co_{0.15}$ $Al_{0.05}$ O_2 Lithium-ion Pouch Cell," *J. Electrochem. Soc.*, vol. 164, no. 7, pp. A1438–A1445, 2017.
[22] V. Marano, S. Onori, Y. Guezennec, G. Rizzoni, and N. Madella, "Lithium-ion batteries life estimation for plug-in hybrid electric vehicles," in *Proc. Vehicle Power Propulsion Conf.*, 2009, pp. 536–543.
[23] M. Swierczynski, D. I. Stroe, A. I. Stan, R. Teodorescu, and D. U. Sauer, "Selection and performance-degradation modeling of LiMo2/Li4Ti5O12 and LiFePO4/C battery cells as suitable energy storage systems for grid integration with wind power plants: An example for the primary frequency regulation service," *IEEE Trans. Sustain. Energy*, vol. 5, no. 1, pp. 90–101, Jan. 2014.
[24] Y. Zhu, F. Yan, J. Kang, C. Du, C. Zhang, and R. F. Turkson, "Fading analysis of the Li(NiCoMn)O2battery under different SOC cycle intervals," *Ionics*, vol. 23, no. 6, pp. 1383–1390, 2017.
[25] J. de Hoog *et al.*, "Combined cycling and calendar capacity fade modeling of a nickel-manganese-cobalt oxide cell with real-life profile validation," *Appl. Energy*, vol. 200, pp. 47–61, 2017.
[26] J. Schmalstieg, S. Käbitz, M. Ecker, and D. U. Sauer, "A holistic aging model for Li(NiMnCo)O2 based 18650 lithium-ion batteries," *J. Power Sources*, vol. 257, pp. 325–334, 2014.
[27] I. Baghdadi, O. Briat, J. Y. Delétage, P. Gyan, and J. M. Vinassa, "Lithium battery aging model based on Dakin's degradation approach," *J. Power Sources*, vol. 325, pp. 273–285, 2016.
[28] I. de la Parra, J. Marcos, M. García, and L. Marroyo, "Control strategies to use the minimum energy storage requirement for PV power ramp-rate control," *Sol. Energy*, vol. 111, pp. 332–343, 2015.
[29] J. Sanchez, "Gestión de la Integración Eólica Masiva en Redes Eléctricas con Almacenamiento de Energía de Litio-Ion," in *Proc. IV Congreso Smart Grids*, 2017, pp. 1–6.
[30] H. Wenzl *et al.*, "Life prediction of batteries for selecting the technically most suitable and cost effective battery," *J. Power Sources*, vol. 144, no. 2, pp. 373–384, 2005.
[31] D. U. Sauer and H. Wenzl, "Comparison of different approaches for lifetime prediction of electrochemical systems—Using lead-acid batteries as example," *J. Power Sources*, vol. 176, no. 2, pp. 534–546, 2008.
[32] A. Barré, B. Deguilhem, S. Grolleau, M. Gérard, F. Suard, and D. Riu, "A review on lithium-ion battery ageing mechanisms and estimations for automotive applications," *J. Power Sources*, vol. 241, pp. 680–689, 2013.
[33] M. Berecibar, I. Gandiaga, I. Villarreal, N. Omar, J. van Mierlo, and P. van den Bossche, "Critical review of state of health estimation methods of Li-ion batteries for real applications," *Renewable Sustain. Energy Rev.*, vol. 56, pp. 572–587, 2016.
[34] J. Wang *et al.*, "Cycle-life model for graphite-LiFePO4cells," *J. Power Sources*, vol. 196, no. 8, pp. 3942–3948, 2011.
[35] D. I. Stroe, M. Swierczynski, A. I. Stan, V. Knap, R. Teodorescu, and S. J. Andreasen, "Diagnosis of lithium-ion batteries state-of-health based on electrochemical impedance spectroscopy technique," in *Proc. Energy Convers. Congr. Expo.*, 2014, pp. 4576–4582.
[36] T. Grün, K. Stella, and O. Wollersheim, "Impacts on load distribution and ageing in Lithium-ion home storage systems," *Energy Procedia*, vol. 135, pp. 236–248, 2017.
[37] S. Panchal *et al.*, "Cycling degradation testing and analysis of a LiFePO4 battery at actual conditions," *Int. J. Energy Res.*, vol. 41, no. 15, pp. 2565–2575, 2017.
[38] B. Weißhar and W. G. Bessler, "Model-based lifetime prediction of an LFP/graphite lithium-ion battery in a stationary photovoltaic battery system," *J. Energy Storage*, vol. 14, pp. 179–191, 2017.
[39] M. J. Swierczynski, "Lithium-ion battery energy storage system for augmented wind power plants," Ph.D. dissertation, Dept. Energy Technol., Aalborg Univ., Aalborg, Denmark, 2012.
[40] S. D. Downing and D. F. Socie, "Simple rainflow counting algorithms," *Int. J. Fatigue*, vol. 4, no. 1, pp. 31–40, 1982.
[41] E. Schaltz, A. Khaligh, and P. O. Rasmussen, "Influence of battery/ultracapacitor energy-storage sizing on battery lifetime in a fuel cell hybrid electric vehicle," *IEEE Trans. Veh. Technol.*, vol. 58, no. 8, pp. 3882–3891, Oct. 2009.
[42] H. Beltran, J. Barahona, R. Vidal, J. C. Alfonso, C. Ariño, and E. Pérez, "Ageing of different types of batteries when enabling a PV power plant to enter electricity markets," in *Proc. Annu. Conf. IEEE Ind. Electron. Soc.*, 2016, pp. 1986–1991.
[43] M. Safari, M. Morcrette, A. Teyssot, and C. Delacourt, "Life prediction methods for lithium-ion batteries derived from a fatigue approach," *J. Electrochem. Soc.*, vol. 157, no. 6, pp. 713–720, 2010.
[44] H. Beltran, M. Swierczynski, N. Aparicio, E. Belenguer, R. Teodorescu, and P. Rodriguez, "Lithium-ion batteries ageing analysis when used in a PV power plant," in *Proc. IEEE Int. Symp. Ind. Electron.*, 2012, pp. 1604–1609.
[45] J. Dambrowski, S. Pichlmaier, and A. Jossen, "Mathematical methods for classification of state-of-charge time series for cycle lifetime prediction," in *Proc. Adv. Automotive Battery Conf.*, 2012, vol. 2018, no. 15, pp. 2–4.
[46] C. M. Hoff and R. Lin, "Development and practical use of a levelized cost of storage (LCOS) metric," NEC Energy, Tokyo, Japan, 2016.
[47] C. S. Lai and M. D. McCulloch, "Levelized cost of energy for PV and grid scale energy storage systems," Sep. 2016. ArXiv preprint arXiv: 1609.06000.
[48] C. Pillot, "The rechargeable battery market and main trends 2016–2025," Avicenne Energy, Paris, France, 2017.
[49] C. Curry, "Lithium-ion battery costs and market," Bloomberg New Energy Finance, New York, NY, USA, 2017.
[50] IRENA, "Electricity storage and renewables: Costs and markets to 2030," Abu Dhabi, UAE, 2017.
[51] J. Mclaren, P. Gagnon, K. Anderson, E. Elgqvist, R. Fu, and T. Remo, "Battery energy storage market: Commercial scale, lithium-ion projects in the U.S.," Nat. Renewable Energy Lab., Golden, CO, USA, 2016.
[52] Lazard, "Lazard's levelized cost of storage analysis— Version 3.0," Hamilton, U.K., 2017.

Hector Beltran received the M.Sc. degree in industrial engineering from the Universitat Jaume I (UJI), Castelló de la Plana, Spain, in 2004, and the Ph.D. degree in electrical engineering from the Technical University of Catalonia (UPC), Barcelona, Spain, in 2011. Since 2006, he has been an Assistant Professor with the Electrical Engineering Area, UJI. His current research interests include massive PV integration into the grid and energy storage systems.

Iván Tomás García received the B.Sc. degree in industrial technology engineering, and the M.Sc. degree in industrial engineering, both from the UJI, in 2015 and 2017, respectively. He is currently working toward the master's degree in management, focused on innovation and internationalization, with UJI.

José Carlos Alfonso-Gil received the M.Sc. degree in automation and industrial electronics engineering from Universitat Politècnica de València (UPV), València, Spain, in 2004, and the Ph.D. degree in electronics engineering in 2010. Since 2007, he has been an Assistant Professor with the Electrical Engineering Area, at UJI. His fields of interest are active power filters, control of power converters, and microgrids.

Emilio Pérez received the M.Sc. degree in industrial engineering from UJI, in 2002, and the Ph.D. degree in control engineering from UPV, in 2011. Since 2006, he has been with the Electrical Engineering Area, UJI, where he is currently an Assistant Professor. His current research interests include control and optimization of PV systems with energy storage, solar forecasting, and lithium-ion batteries, ageing and management.